Underwater GPS System
for Autonomous Underwater Wireless Drone Control

Yukiko Muller[1], Shiho Oshiro[1], Shigeo Nakagawa[2], and Tomohisa Wada[3]

1) Graduate School of Engineering and Science, University of the Ryukyus, Senbaru 1, Nishihara, Okinawa Japan
2) Cyohemon GK, Kamogawa-cho 14-1-519, Mishima-shi, Shizuoka, Japan
3) Dept. of Engineering, University of the Ryukyus, Senbaru 1, Nishihara, Okinawa Japan

Abstract

This research describes an underwater positioning system for swarming multiple AUVs. The existing Global Positioning System satellite (GPS) constellation provides limited availability and reliability. Thus, it is of interest to examine GPS using the integrated GNSS advantage. The purpose is to explore the usage underwater and subsurface monitoring, drone-based monitoring, digital forensic environment, and other defense-related applications. With the Long Base Line (LBL) technique, the proposed system contains three and four known reference points. And as a result, an LBL underwater acoustic positioning system is ideal for low-cost autonomous underwater AUV control. This is a cutting-edge technique for technical application that will allow the drone to inspect the ship and detect any damage by scanning the submerged surface of marine ships and receiving accurate damage position information. Using this system, we can achieve a more accurate positions for the three and four reference points. A computer-based signal processing comparison of 3 BS vs 4 BS: Four scenarios were simulated, with the SL's Carrier to Noise to Ratio CNR=0dB and the DL's CNR dB=6dB and CNR=0dB and the DL's CNR dB=6dB.

Keywords:
Underwater GPS, Underwater Positioning, Underwater Communications, Underwater applications

1. Introduction

Aerial/Underwater drone is an autonomous robot capable of traveling and working across the air surface and underwater [1]. Due to the technological restriction's exploration, it has been a hot topic for research. The examination of drone behaviors is important. Recent improvements in object recognition have combined cutting-edge technology with advanced intelligent control strategies to extract high-level information for object detection. The Global Navigation Satellite System (GNSS) is ineffective underwater, it is therefore necessary to have a particular underwater positioning system [2]. Underwater robots are designed to work as an alternative to humans because of a difficult and hazardous underwater environment. These designs are built on open-source hardware to contribute to manufacturing innovation, including drones [3]. In our project design, the underwater drone was created by extending the Raspberry Pi computer module, using Xilinx

Zynq ARM-embedded FPGA chip as our system board and the transducer is based on an Oki Seatec OST2120[4].

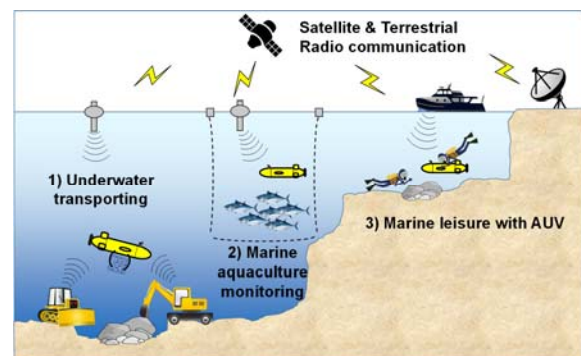Fig. 1 depicts the overview of the communication system

Fig. 1: Applications for Underwater Drones

for underwater positioning and the applications for the underwater drones. Drone technology has advanced to the point where they can be used in a wide range of applications such as underwater transporting, marine aqua-culture monitoring, and marine leisure in which those drones are primarily used in unmanned aerial vehicles. The basic goal of this technology is to connect the physical and virtual worlds at any time and from any location. It aims to create a world of convenience for all that includes living humans, physical items, virtual data, and the environment [5].
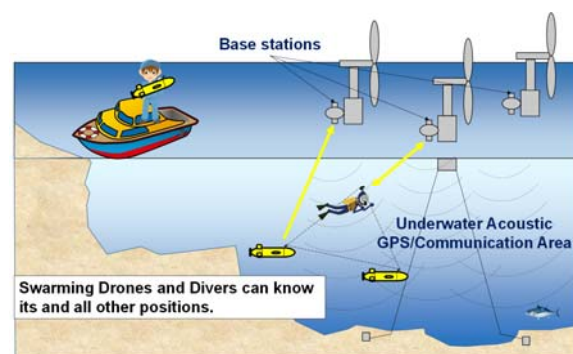

Fig 2. Underwater GPS for Swarming AUVs

Fig. 2 displays an underwater GPS for swarming AUVs. This overall concept of the positioning system has multiple base stations. Both the swarming AUVs and divers can determine the system's reference points, in other words, they can know its/others positions. Along with that, all the BS can be synced by GNSS. The proposed system refers to the depth information and distances between the AUVs.

The undersea environment is vital, especially for commercial divers. Divers' labor is particularly dangerous because of its length and complexity. Because the application employed in it are so limited, this issue is frequently overlooked. But an accurate evaluation of the system is a necessity for tackling difficulties linked with surf zone variability, which can affect human activities underwater. As a result, constant monitoring is a huge difficulty, especially when using a new environmentally friendly system. With this proposed system, these applications are capable to achieve this target.
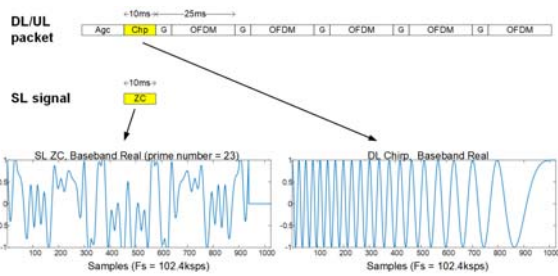
2. OPERATIONS

Fig. 3: Down Link and Side Link Signals

Down Link (DL) and Side Link (SL) signal packets are shown in Fig. 3 as the signaling packets and timing detection Reference Signals. DL includes the Chirp signal 'A' as well as the OFDM communication signal because it can be easily recognized under the Doppler shift situations [6]. The Zadoff-Chu (ZC) sequence is used to recognize those SL signals in overlapping settings because SL is made up of only one 10ms detecting signal. ZC sequences signal
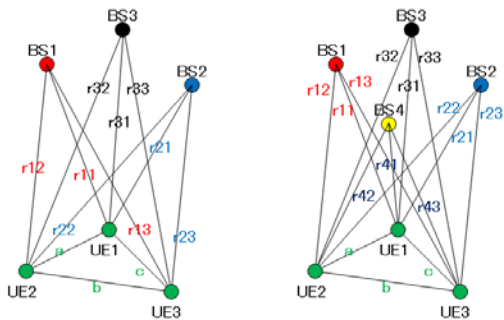

Fig. 4: 3 and 4 Base Stations Distances

C, D, E, F, G, H, J, K, and L each correlate to a distinct prime number.

Fig. 4 depicts the topology relationship for the distances between all the nodes in the system that measured by the system that has been determined via DL and SL signals. Base Station and User Equipment, respectively, are abbreviated as BS and UE.
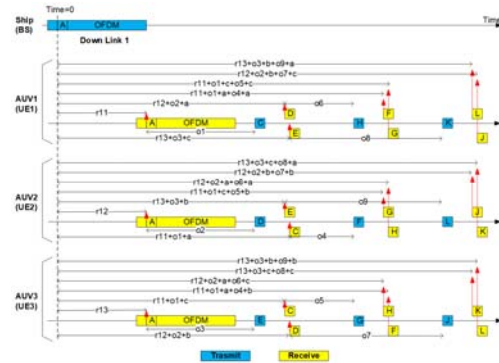

Fig. 5: Down Link and Side Link Timing Diagram

Each AUV detects signal 'A' and sends it to signal C, D, or E to the other AUVs with the delay of o1, o2, or o3. The timings are indicated by the red arrow in Fig.5 that can be estimated by detecting the C, D, and E signals from the neighboring AUVs. Each AUV has seven timings that have been measured. All the timings, that are the red arrows pointing up, can be measured by repeating the Side Link two more times with the signals of F, G, H, J, K, and L. There are six distances, which are the delay times such as r11, r12, r13, a, b, and c, that can be solved independently in each AUV that is utilizing those mentioned seven timings. Repeatedly, the same process will be performed by another Down Link from the other BS allowing, r21, r22, r23, a, b, and c, the distances to be calculated. Consequently, the position of the AUV cannot be determined by only measuring these distances. On the other hand, the sets of the UE positions can be solved by considering the depth of each UE. According to the two sets, the UE's fixed-triangle position sequence can be classified as Clockwise (CW) or Counterclockwise (CCW) [7]. In order to obtain one position solution to set the CW or CCW, the rotation sequence has to be known in which each UE has a function that can detect the position of the other UEs.

The Underwater Positioning System's detailed parameters are shown in Table 1. The acoustic signal has an 8kHz bandwidth and a 16kHz central frequency. With a Guard Interval of 5.0ms, the 2048-point OFDM symbol length is 20.0ms. The total number of sub carriers is 161, with a sub carrier spacing of 50kHz. With the QPSK modulation and R=1/2 Convolutional Code forward error correction, the 5 OFDM symbol packet size carries 596-bit data [8].

Table 1: Underwater Positioning System Parameters

Parameters	Values
Signal Band	16kHz±4kHz
Sampling Frequency	102.4k Hz
DL reference signal	10.0ms Chirp
SL reference signal	10.0ms Zadoff-Chu (N_{ZC}=73)
OFDM symbol length T	20.0 ms (2048 points)
FFT Size	2048
GI length Tg	5.0 ms (512 points)
Effective Symbol length Tu=T+Tg	25.0 ms
Sub Carrier Spacing	50.0 Hz
Number of Sub Carrier	161
Number of Pilot in OFDM symbol	Zadoff –Chu, N_{ZC}= 81 and 13
Down Link OFDM packet size	5 OFDM symbols
Forward Error Correction	Convolution Code (k=7, R=1/2)
Sub Carrier Modulation	QPSK
Packet Data Size	596 bit

3. SYSTEM DESIGN

The total system utilizes the same H/W of two reference points BS system [8]. Fig. 6 depicts the signal processing on the BS side. The System Design, with a Passband of 16kHz, for both the transmitting (BS1 TX) and the receiving (BS1 RX) functions are available on the BS side. Because the signal transmission from the UE to the BS consumes relatively high power compared to the SL power, the receiver must monitor the condition of the UE at the extended intervals. The only function for the BS is to generate the DL signal with GNSS information that is embedded in it. Therefore, the receiver must monitor the
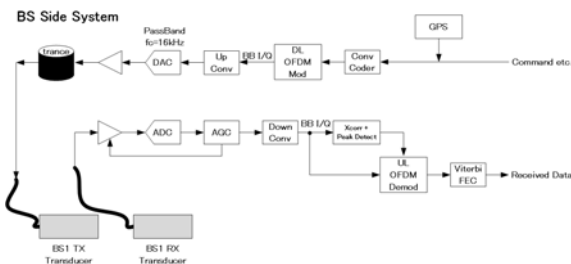

Fig. 6: BS Side Signal Processing Block Diagram

Fig. 7: UE Signal Processing Block Diagram

condition of the UE at the extended intervals as signal transmission from the UE to the BS which requires comparatively high power when compared the to the SL powers.

The signal processing diagram on the UE side is shown in Fig. 7. A two-element transducer have been recently designed. For the OFDM transmission, the Ha branch is used for the RX and the TX. SL signals are detected using both the Ha and Hb branches. Not only are they the exact timings recorded for the distance measurement, but they are also the phase for the difference between the receiving SL signals that have been detected to obtain directional information. This function will be used to set the fixed-triangle placement of the UEs CW or CCW. With 11 templates, such as 'A' as chirps, C to L for the 9 ZC sequences, and the Ha and Hb receivers with the matched filters as the cross correlator.
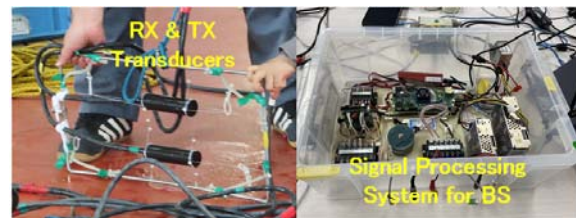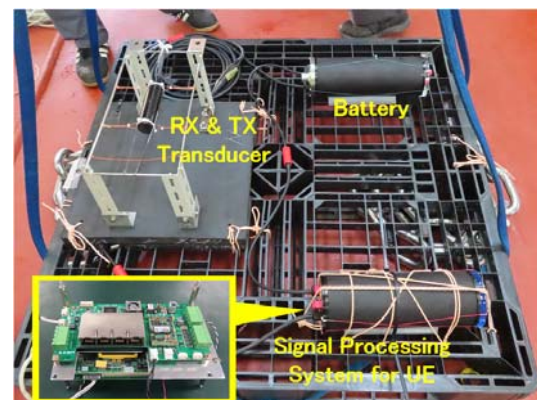

Fig. 8: Mother ship (BS) side System

Fig. 9: AUV (UE) side System

The image for the two-element transducer is shown in Fig. 8. One transducer for the RX and TX and the other one is for the signal processing system for the BS. The transducer is based on an Oki Seatec OST2120 transducer with Ha/Hb two branches that merged into one body. The signal processing system is employed by a Zynq7000 ARM-embedded FPDG and an OST7010 Power Amplifier that powers the TX transducer via the transformer.

The System Board for the UEs is employed by a Xilinx Zynq ARM-embedded FPGA chip is shown in Fig. 9. For the 16QAM modulation with the code rate of R=1/2, one UL frame may send 3790 bytes and for the QPSK modulation with the code rate of R=1/2, one UL frame can transfer 1895 bytes. Fig. 9 shows a snapshot of the modem H/W system.

4. CALCULATIONS

To determine the user's position in three dimensions (x_u, y_u, z_u) as well as the offset t_u, pseudo range measurements are made to the satellites resulting in the system of equations. The equation may be expanded into a set of equations in the unknown (x_u, y_u, z_u) and (t_u); whereas x, y, and z can denote the user's coordinates (x_u, y_u, z_u) in addition to the receiver clock offset in which t_u is then calculated. As long as the displacement are within close proximity of the linearization point, the linearization scheme can work well [9].

The targeting system area is within a fixed-triangle area with 3 and 4 four reference points (BS1, BS2, BS3, BS4) and 3 AUVs (UE1, UE2, UE3) as shown in Fig. 10-12. The system consists of an OFDM-based DL and SL communication functions, commands, and distance measurement nodes. It also consists of a special sequence that includes the chirp between the BS and the UEs as Down Link and Zadoff-Chu (ZC) sequence between the UEs as Side Link. A detailed computer-based signal processing simulation has resulted that for every UE, the UE's position can be identified on its own and also for the additional UEs' positions. But keep in mind that in reality, the true user-to-satellite measurements are corrupted by uncommon errors, such as measurements noise, deviation of satellite path from the reported ephemeris, and the multipath.

5. COMPUTER SIMULATIONS

The simulated signal waveforms are depicted in Fig. 14-16., where the time axis varies from 0.2 to 6 seconds between the BS and the UE placements. A propagation delay of approximately 0.2 seconds is necessary due to the free-depth information. Simply put, in the simulation, the time between all the BS is 0.2 seconds. For each example, the control delays of o1 to o9 are best set. Though the Down
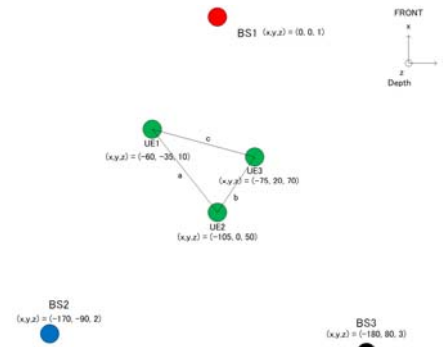

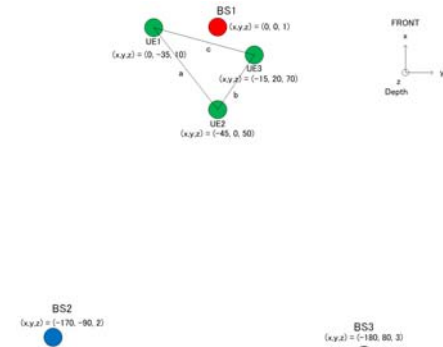Fig. 10: BS and UE placement for 3A

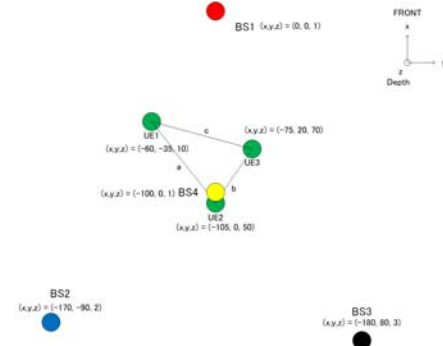Fig. 11: BS and UE placement for 3B

Fig. 12: BS and UE placement for 4A

Fig. 13: BS and UE placement for 4B

Link and its activities are not depicted in the diagrams, the TX signals are represented by the red waves.

The performance of the simulated Down Link OFDM Packet Bit Error Rate is displayed in Fig. 17. The Forward error correction is achieved by using the QPSK sub carrier modulation and a Convolutional encoder with the Constraint length of K=7 and the Code Rate of R=1/2. The Soft decision Viterbi decoder is employed on the receiver's side. The Error-free operation is accomplished when the Carrier Power to Noise Ratio (CNR) is greater than 6dB. Then the DL CNR of 6dB is used in the subsequent SL simulations.

The simulated placement errors for 4 cases are shown in Fig. 18-21. In the proposed system, the positions of the 3 and 4 AUVs are estimated in each AUV. The figures show the positioning errors of the three UEs as computed by UE2. The position 'UE2' can be estimated by combining the lengths of r12 and r22 with the depth of UE2 as described
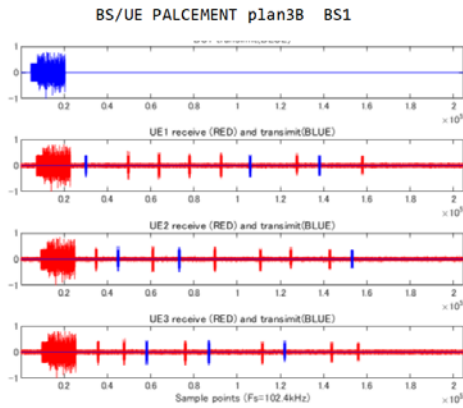
Fig. 14: Simulated Waveform for BS1
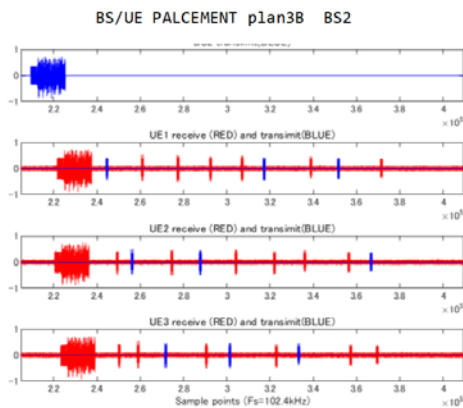
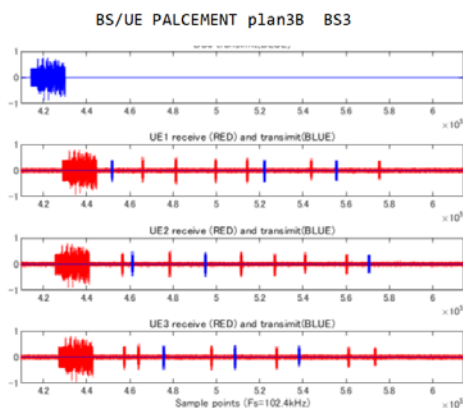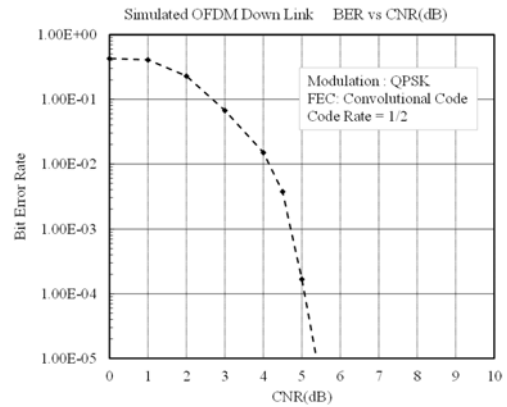Fig. 15: Simulated Waveform for BS2

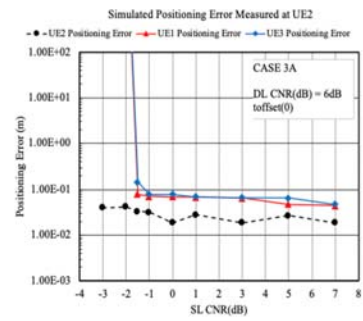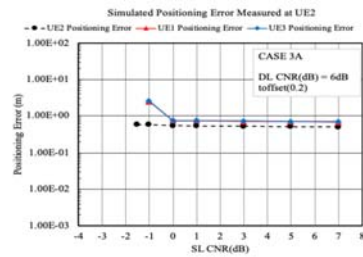Fig. 16: Simulated Waveform for BS3

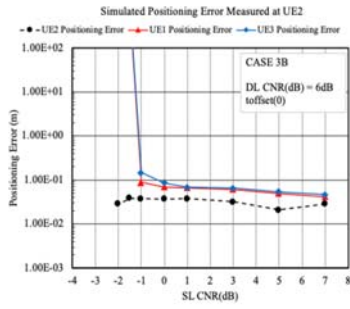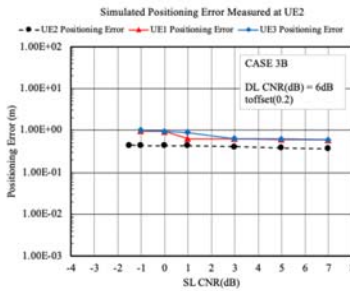Fig. 17: Simulated OFDM Down Link: BER vs CNR (dB)

(a) toffset=0

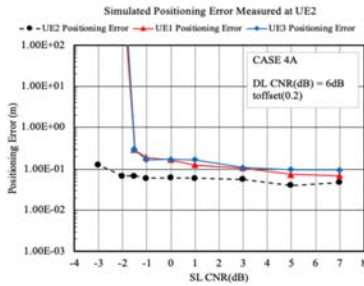(b) toffset=0.2

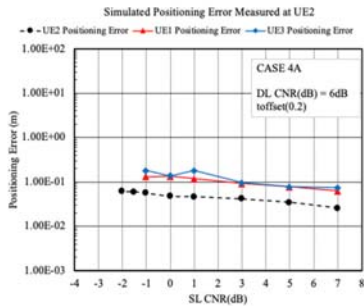Fig. 18: Simulated Positioning Error for 3A

(a) toffset=0

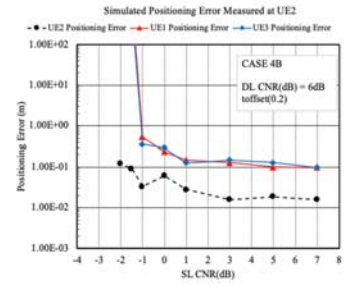(b) toffset=0.2

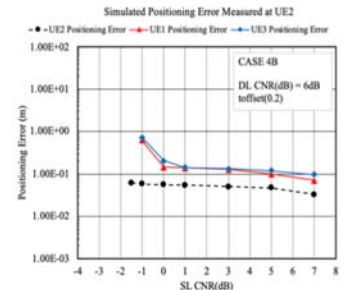Fig. 19: Simulated Positioning Error for 3B

(a) toffset=0

(b) toffset=0.2

Fig. 20: Simulated Positioning Error for 4A

(a) toffset=0

(b) toffset=0.2

Fig. 21: Simulated Positioning Error for 4B

(a) CASE 3A and 4A
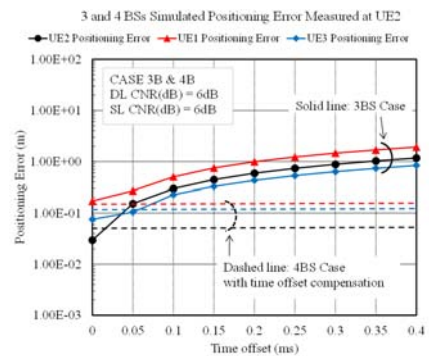
(b) CASE 3B and 4B

Fig. 22: Simulated Positioning Error for 3A-B; 4A-B

in the calculations section. Because the positioning error of UE2 is independent of the SL_CNR (dB), Fig. 18-19 depicts UE2's flat features, while in Fig. 20-21, the offset (t_u) is also independent. All measured lengths, such as r11, r12, r13, r22, r23, a, b, and c, determine the UE1 and UE3 positioning errors, which means they rely on the SL_CNR (dB) for the two-positioning error.
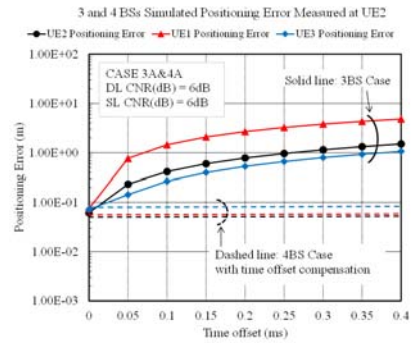
Because the simulations assume the acoustic sound propagation speed, which is a function of ambient temperature salinity, and water pressure is accurately approximated, the simulation results have shown a lower bound in the system for the positioning error in Fig. 22 by using the MMSE calculation.

To further elaborate, an assumption was made in regard to changing the time offset (t_u) as shown in the figures provided for 'Simulated Positioning Error' in the Computer Simulations section. In Fig. 18 (3A) & Fig. 19 (3B) we set dB=6; and (t_u)=0ms & 0.2ms. We must also take into account that the UEs time error is at 0.2/8hrs. Not only that but having the same time offset (t_u) as shown in Fig. 20 (4A) & Fig. 21 (4B) where dB=6; and (t_u)=0.2ms & 0.2ms for comparison was also computed.

5. Conclusions

For multiple swarming AUVs, this paper described and compared a 3 and 4 Reference Point Underwater Positioning System. The Long Base Line (LBL) approach requires more than three known reference points, which has been conducted in the above work. Our work demonstrates that the system's reference points can be adjusted, all the BS can be synced by GNSS, and 3 UEs can identify its/other UE positions.

For the calculation, the nonlinear equation can be solved for the unknowns by employing iterative techniques based on linearization. If we know approximately where the receiver is, then we can denote the offset of the true position (x_u, y_u, z_u) from the approximate position by a displacement. By expanding the approximate position, we can obtain the position offset as a linear function of the known coordinates and pseudo range measurements.

Fig. 22 indicates the improvements that are made when having four reference points. In comparison to the 3 BS case, the 4 BS case can achieve a more accurate position because of the additional capability. It means that the time offset can be precisely estimated. As seen in the provided figures in the computer simulation's section for the positioning error, the 4 BS cases are better than the 3 BS cases.

Acknowledgments

References

[1] M. Sasano, S. Inaba, A. Okamoto, T. Seta, K. Tamura, T. Ura, S. Sawada, and T. Suto, "*Development of a Regional Underwater Positioning and Communication System for Control of Multiple Autonomous Underwater Vehicles*," (2016)

[2] *Underwater Acoustic Positioning Systems*, Chapter 4. P.H Milne, 1983, ISBN 0-87201-012-0

[3] Y. He, D.B. Wang, and Z.A A, "*A review of different designs and control models of remotely operated underwater vehicle*," (2020)

[4] Y. Muller, S. Oshiro, T. Motohara, A. Kinjo, T. Suzuki, and T. Wada, "*Underwater Acoustic Mavlink Communication for Swarming AUVS*," (2021)

[5] V.S Kodogiannis and J. Lygouras, "*Special Issue: Unmanned Underwater Vehicles (UUV)-Advances, Applications & Challenges*," (2021)

[6] T. Wada, T. Suzuki, H. Yamada, and S. Nakagawa, "*An Underwater Acoustic 64QAM OFDM Communication System with Robust Doppler Compensation*," MTS/IEEE OCEANS (2016)

[7] T. Wada, S. Nakagawa, A. Kawamori, T. Suzuki, and H. Toma, "*Two Reference points Underwater Positioning System for Swarming AUVs Team Operation*," (2021)

[8] T. Moon, *ERROR CORRECTION CODING Mathematics Methods and Algorithm*, WILEY, pp.453-486 (2005)

[9] E.D. Kaplan, C.J. Hegarty, "*Understanding GPS PRINCIPLES AND APPLICATIONS*," Second Edition (2006)